Standing waves between immiscible liquids inside an infinite boxed basin

2008 J. Phys. A: Math. Theor. 41 175501

(http://iopscience.iop.org/1751-8121/41/17/175501)

IOP PUBLISHING JOURNAL OF PHYSICS A: MATHEMATICAL AND THEORETICAL

J. Phys. A: Math. Theor. **41** (2008) 175501 (21pp) doi:10.1088/1751-8113/41/17/175501

Standing waves between immiscible liquids inside an infinite boxed basin

Kadry Zakaria

Department of Mathematics, Faculty of Science, Tanta University, Tanta, Egypt

Received 2 October 2007, in final form 10 January 2008
Published 15 April 2008
Online at stacks.iop.org/JPhysA/41/175501

Abstract

Faraday waves with three modes, on the interface between superposed liquids in an infinite boxed basin subjected to vertical excitation, were studied. The longitudinally exciting acceleration is decomposed into two modes. The solutions are constructed using the method of multiple timescales. The solvability conditions are exploited to derive a system of nonlinear autonomous six-order ordinary differential equations governing the modulation of the amplitudes and phases of the resonated waves. These equations have been used to determine steady-state solutions and hence their stability. The conditions of existence of both regular periodic and chaotic regimes are obtained analytically and in numerical applications pictures.

PACS number: 47.10.−g

1. Introduction

The motion of liquid with a free surface is of great concern in many engineering disciplines such as fuel sloshing of rocket propellant, oil oscillation in large storage tanks, water oscillation in reservoirs due to an earthquakes, sloshing of water in pressure-suppression pools of boiling water reactors and several others.

The first research describing standing waves caused by a forcing whose frequency was twice a resonance frequency was done by Michael Faraday [1]. He observed that when a water-filled basin is placed on a plane that oscillates vertically with approximately twice a resonance frequency, waves are generated on the surface. By introducing a coordinate system moving with the basin, we can interpret this problem as that of a stationary basin with oscillating gravity. In the literature, these waves are named 'Faraday waves' after their first observer. Faraday waves have been discussed by [2–8] and others. While the phenomenon of Faraday waves may be one of the most famous, water wave phenomena in a basin had certainly been observed long before. Standing waves of a high resonance frequency corresponding to an asymmetric mode were observed when the forcing frequency was close to that high resonance frequency. If the forcing frequency was increased and close to the sum of that high frequency

and the lowest frequency of axisymmetric modes, waves of that low frequency were observed as well. Self-excited vibration of shell-liquid coupled systems were discussed by Liu *et al* [9]. It was shown by Sun *et al* [10] that for an asymmetric mode by itself the center of the surface is very calm, whereas the center of the region is where the maximum amplitude for an axisymmetric mode is observed. These observations motivated more theoretical studies. An exact solution of the linearized problem of harmonic forcing applied to the side walls of a circular basin was found by Shen *et al* [11].

Nonlinear amplitude equations are often used to model Faraday waves. The weakly nonlinear problem was discussed in [12] under the assumption that the forcing was close to a resonance frequency or twice the fundamental frequency. A multi-scale asymptotic expansion approach was used to find the equations governing surface waves in each of these cases. It was shown that the amplitude of such surface waves is bounded, except when twice the fundamental frequency also happens to be a resonance frequency. Several recent papers have emphasized the significance of nonlinear terms (cubic in the wave amplitude) in these equations, showing that their retention in the model is often vital to successfully describe hysteresis in Faraday waves (Milner [13], Craik and Armitage [14], Decent [15] and Decent and Craik [16]), pattern selection (Miles [17]) and sideband instability (Decent and Craik [18, 19]). The coefficients, and particularly the signs of the coefficients, of these cubic terms have been shown to be critical to the behavior of Faraday waves. The role of resonant triad interactions in the formation of Faraday wave patterns has been investigated extensively by Vinals and co-workers for both the cases of single frequency forcing [20, 21] and two-frequency forcing [22]. The most detailed two-frequency calculations focused on the situation where the frequency ratio was $\frac{1}{2}$, and the onset surface wave response was subharmonic with the forcing. Zhang and Vinals [21] compared their theoretical results with the experimental results of Muller [23], who observed subharmonic hexagons, triangles and squares near the bicritical point—which pattern was observed depending on a relative phase between the frequency ω and 2ω sinusoidal waveforms in the forcing function.

Some research that deals with rectangular containers was done by Huntley [24] and Mahony and Smith [25]. In [25], the deep water problem for a rectangular organ pipe is considered. The flow field was assumed to be two dimensional. It was shown that surface water waves may be excited by high-frequency acoustic fields. More recently, Yoshimatsu and Funakoshi [26] investigated the resonance waves in square containers caused by horizontal oscillations. It was shown that the kind of waves observed depends on the angle of the direction of oscillation with a container wall. A weakly nonlinear theory [27] has been developed by an asymptotic approach for excited capillary-gravity waves in a water-filled two-dimensional rectangular basin under some edge condition at the contact line. In that study, they assumed that the forcing frequency is near a resonance frequency or some combination of the resonance frequencies. By using a two timescale asymptotic expansion of the solution and solvability conditions for the equations of the third-order approximations in the expansion, the amplitude equations of the excited surface waves at the resonance frequencies are derived.

The problem considered here concerns linear and nonlinear surface waves under the action of a harmonic forcing together with the influence of gravity and surface tension in a two-dimensional rectangular basin. The frequency of the forcing is assumed to be close to a resonance frequency or some combination of the resonance frequencies. The outline of the paper is as follows: in section 2, we describe the physical problem and give the exact dimensionless equations as well as the dispersion equations. Section 3 is devoted to developing the asymptotic solution, using multiple timescales, that leads to the modulation equations in the resonance cases and to obtaining the analytical solutions of the fixed points as well as

the stability conditions. Section 4 contains the numerical results, and finally conclusions are given in section 5.

2. Formulation of the problem

Consider two incompressible immiscible semi-infinite fluids inside an infinite rectangular box. The motion is assumed to be represented by potential functions (according to the viscous potential flow theory [28–30]. Let (x, y) and z be the horizontal and vertical fixed reference coordinates of a rectangular infinite container C having a cross-section S which is assumed to be independent of z, and with $\mathbf{n}$ being an outward vector normal to C. The z-axis is positive inside the upper liquid. The distance, the time and the velocity potential ϕ_j are made dimensionless using $\left(\frac{T}{g\rho_1}\right)^{\frac{1}{2}}$, $\left(\frac{T}{g^3\rho_1}\right)^{\frac{1}{4}}$ and $\left(\frac{T}{g^{\frac{1}{3}}\rho_1}\right)^{\frac{3}{2}}$, respectively, where g is the gravity assumed to be acting along the negative z-axis and T is the surface tension. The quantities ρ_1 and ρ_2 are the densities of the lower and upper fluids, respectively.

The basic equations that govern the perturbed velocity potential ϕ_j with the boundary conditions are

$$\nabla^2\phi_j = 0, \qquad j = 1, 2, \tag{1}$$

$$\frac{\partial\phi_j}{\partial z} = \frac{\partial\eta}{\partial t} + \nabla_{xy}\eta\cdot\nabla_{xy}\phi_j, \qquad z = \eta, \quad j = 1, 2, \tag{2}$$

$$\begin{aligned}\rho\left(\frac{\partial\phi_2}{\partial t} + \frac{1}{2}|\nabla\phi_2|^2\right) - \left(\frac{\partial\phi_1}{\partial t} + \frac{1}{2}|\nabla\phi_1|^2\right) + (\rho-1)(1 + f_1\cos(\Omega_1 t) + f_2\cos(\Omega_2 t))\eta \\ + 2\tilde{\mu}_2\left(\frac{\partial^2\phi_2}{\partial z^2} - \frac{\partial\eta}{\partial x}\frac{\partial^2\phi_2}{\partial x\partial z} - \frac{\partial\eta}{\partial y}\frac{\partial^2\phi_2}{\partial x\partial z}\right) \\ - 2\tilde{\mu}_1\left(\frac{\partial^2\phi_1}{\partial z^2} - \frac{\partial\eta}{\partial x}\frac{\partial^2\phi_1}{\partial x\partial z} - \frac{\partial\eta}{\partial y}\frac{\partial^2\phi_1}{\partial x\partial z}\right) + \nabla^2_{xy}\eta \\ = 0, \qquad z = \eta, \quad j = 1, 2,\end{aligned} \tag{3}$$

where $\rho = \rho_2/\rho_1$, f_1 and f_2 are called the forcing amplitudes of the oscillating external forces, and $\tilde{\mu}_j = \mu_j\left(\frac{1}{gT^3\rho_1}\right)^{\frac{1}{4}}$, since $\mu_{1,2}$ are the viscosity coefficients.

The solution of (1) that satisfies (2) and (3) is

$$\phi_j = \sum_n A_{jn}(t)\psi_n(x, y)\,\mathrm{e}^{(-1)^j k_n z}. \tag{4}$$

The eigenfunction $\psi_n(x, y)$ satisfies the equation

$$\nabla^2_{xy}\psi_n + k_n^2\psi_n = 0 \tag{5}$$

with the boundary condition

$$\nabla\psi_n\cdot\mathbf{n} = 0 \quad \text{on} \quad C, \tag{6}$$

where

$$\iint \psi_n\psi_m\,\mathrm{d}S = \delta_{nm}S \tag{7}$$

and S is the box cross section and the considered container of dimensionless length M by N. We can put the interfacial elevation in the form

$$\eta = \sum_n \zeta_n(t)\psi_n(x, y). \tag{8}$$

Expanding all the boundary conditions at the interface $z = \eta(x, y, t)$ about $z = 0$ using Maclaurin's series and substituting equations (4) and (8) into theses conditions and using the orthonormality condition, we have the following dispersion equations:

$$\ddot{\zeta}_n + \frac{2(\tilde{\mu}_1 + \tilde{\mu}_2)}{1+\rho}\dot{\zeta}_n + \frac{(N^2\pi^2 + M^2\pi^2 - N^2M^2(\rho-1))k_n}{N^2M^2(1+\rho)}\zeta_n + \frac{(1-\rho)(f_1\cos(\Omega_1 t) + f_2\cos(\Omega_2 t))k_n}{1+\rho}\zeta_n + \chi_n = 0. \tag{9}$$

In the case of three modes, we put $\zeta_n(t) = 0$ for $n \geqslant 4$. The quantity χ_n is a function of $\zeta_1(t)$, $\zeta_2(t)$, $\zeta_3(t)$ and their derivatives.

3. The solution method

In this work, we study the behavior of the three modes of interfacial Faraday waves caused by the vibration of a container. The method of multiple timescales will be used to determine a second-order uniform expansion of the solution of equations (9) for small but finite amplitudes in the resonance cases: (1) $\omega_1 + \omega_2 = \omega_3 + \epsilon\sigma_1$, $\Omega_1 = 2\omega_1 + \epsilon\hat{\sigma}_1$, and $\Omega_2 = 2\omega_2 + \epsilon\hat{\sigma}_2$. (2) $\omega_2 + \omega_3 = \omega_1 + \epsilon\sigma_2$, $\Omega_1 = 2\omega_2 + \epsilon\hat{\sigma}_3$ and $\Omega_2 = 2\omega_3 + \epsilon\hat{\sigma}_4$. The detuning parameters $\sigma_{1,2}$ and $\hat{\sigma}_{1,2,3,4}$ have been used to express the nearness of the suggested resonance cases.

We assume the forcing amplitudes f_j and the viscosity numbers $\tilde{\mu}_j$ to be an $\bigcirc(\epsilon)$ quantity ($\epsilon \ll 1$) so that $f_j = \epsilon\delta_j$ and $\tilde{\mu}_1 + \tilde{\mu}_2 = \epsilon\hat{\mu}_\ell$. We introduce a long timescale t_1 by means of the substitution $\frac{\partial}{\partial t} \to \frac{\partial}{\partial t} + \epsilon\frac{\partial}{\partial t_1}$. We expand the interfacial elevation in powers of ϵ as

$$\zeta_n = \epsilon\zeta_{1n}(t, t_1) + \epsilon^2\zeta_{2n}(t, t_1) + \cdots. \tag{10}$$

Substituting equation (10) into equations (9), the solution of the first-order problem can be expressed in the form

$$\zeta_{1n} = A_n(t_1)\,\mathrm{e}^{\mathrm{i}\omega_n t} + \bar{A}_n(t_1)\,\mathrm{e}^{-\mathrm{i}\omega_n t}, \tag{11}$$

where $\bar{A}_n(t_1)$ is the complex conjugate of $A_n(t_1)$, and

$$\omega_n^2 = \frac{(N^2+M^2)\pi^2 + M^2N^2(1-\rho)}{M^2N^2(1+\rho)}. \tag{12}$$

3.1. Modulation equations

Substituting equations (10) and (11) into equations (9) and eliminating the terms that produce secular terms, in cases of resonance, we have the following solvability conditions.

3.1.1. The first resonance case.

$$\mathrm{i}\dot{A}_1 + \mathrm{i}\alpha_1 A_1 + \alpha_2\,\mathrm{e}^{\mathrm{i}\hat{\sigma}_1 t_1}\bar{A}_1 + \alpha_3\,\mathrm{e}^{\mathrm{i}\sigma_1 t_1}\bar{A}_2 A_3 = 0, \tag{13}$$

$$\mathrm{i}\dot{A}_2 + \mathrm{i}\beta_1 A_2 + \beta_2\,\mathrm{e}^{\mathrm{i}\hat{\sigma}_2 t_1}\bar{A}_2 + \beta_3\,\mathrm{e}^{\mathrm{i}\sigma_1 t_1}\bar{A}_1 A_3 = 0, \tag{14}$$

$$\mathrm{i}\dot{A}_3 + \mathrm{i}\gamma_1 A_3 + \gamma_2\,\mathrm{e}^{-\mathrm{i}\sigma_1 t_1}A_1 A_2 = 0. \tag{15}$$

3.1.2. The second resonance case.

$$\mathrm{i}\dot{A}_1 + \mathrm{i}\alpha_1 A_1 + \alpha_4 \,\mathrm{e}^{\mathrm{i}\sigma_2 t_1} A_2 A_3 = 0, \tag{16}$$

$$\mathrm{i}\dot{A}_2 + \mathrm{i}\beta_1 A_2 + \beta_4 \,\mathrm{e}^{\mathrm{i}\hat{\sigma}_3 t_1} \bar{A}_2 + \beta_3 \,\mathrm{e}^{-\mathrm{i}\sigma_2 t_1} A_1 \bar{A}_3 = 0, \tag{17}$$

$$\mathrm{i}\dot{A}_3 + \mathrm{i}\gamma_1 A_3 + \gamma_3 \,\mathrm{e}^{\mathrm{i}\hat{\sigma}_4 t_1} \bar{A}_3 + \gamma_4 \,\mathrm{e}^{-\mathrm{i}\sigma_2 t_1} A_1 \bar{A}_2 = 0, \tag{18}$$

where $\dot{A}_n = \frac{\mathrm{d}A_n}{\mathrm{d}t_1}$.

The quantities α's, β's and γ's are given in the appendix.

3.2. Fixed points

In this paper, we discuss the first case of resonance in detail, and similarly the other case can be investigated. To investigate the solution of equations (13)–(15), it is convenient to express the complex amplitudes of the three modes of the resonant waves in the polar form

$$A_j = a_j \,\mathrm{e}^{\mathrm{i}\Upsilon_j}, \qquad j = 1, 2, 3 \tag{19}$$

where the a_j and Υ_j are the modified real amplitudes and phases of the three modes. Substituting equation (19) into equations (13)–(15) and separating the real and imaginary parts, we then have

$$\frac{\mathrm{d}a_1}{\mathrm{d}t_1} + \alpha_1 a_1 + \alpha_2 a_1 \sin\psi_1 + \alpha_3 a_2 a_3 \sin\psi_2 = 0, \tag{20}$$

$$-a_1 \frac{\mathrm{d}\Upsilon_1}{\mathrm{d}t_1} + \alpha_2 a_1 \cos\psi_1 + \alpha_3 a_2 a_3 \cos\psi_2 = 0, \tag{21}$$

$$\frac{\mathrm{d}a_2}{\mathrm{d}t_1} + \beta_1 a_2 + \beta_2 a_2 \sin\psi_3 + \beta_3 a_1 a_3 \sin\psi_2 = 0, \tag{22}$$

$$-a_2 \frac{\mathrm{d}\Upsilon_2}{\mathrm{d}t_1} + \beta_2 a_2 \cos\psi_3 + \beta_3 a_1 a_3 \cos\psi_2 = 0, \tag{23}$$

$$\frac{\mathrm{d}a_3}{\mathrm{d}t_1} + \gamma_1 a_3 - \gamma_2 a_1 a_2 \sin\psi_2 = 0, \tag{24}$$

$$-a_3 \frac{\mathrm{d}\Upsilon_3}{\mathrm{d}t_1} + \gamma_2 a_1 a_2 \cos\psi_2 = 0, \tag{25}$$

where $\psi_1 = -2\Upsilon_1 + \hat{\sigma}_1 t_1$, $\psi_2 = -\Upsilon_1 - \Upsilon_2 + \Upsilon_3 + \sigma_1 t_1$, $\psi_3 = -2\Upsilon_2 + \hat{\sigma}_2 t_1$.

In order to demonstrate the steady-state response of the system under consideration, we must determine the fixed points of equations (20)–(25). However, these will be obtained by setting $\frac{d\{a_j, \psi_j\}}{\mathrm{d}t_1} = 0$.

Then, it follows that

$$\frac{\mathrm{d}\Upsilon_1}{\mathrm{d}t_1} = \frac{1}{2}\hat{\sigma}_1, \qquad \frac{\mathrm{d}\Upsilon_2}{\mathrm{d}t_1} = \frac{1}{2}\hat{\sigma}_2, \qquad \frac{\mathrm{d}\Upsilon_3}{\mathrm{d}t_1} = \frac{1}{2}(\hat{\sigma}_1 + \hat{\sigma}_2) - \sigma_1. \tag{26}$$

Hence the triple (a_1, a_2, a_3) will be obtained by solving the following system of algebraic equations:

$$\alpha_1 a_1 + \alpha_2 a_1 \sin\psi_1 + \alpha_3 a_2 a_3 \sin\psi_2 = 0, \tag{27}$$

$$-\tfrac{1}{2}\hat{\sigma}_1 a_1 + \alpha_2 a_1 \cos\psi_1 + \alpha_3 a_2 a_3 \cos\psi_2 = 0, \tag{28}$$

$$\beta_1 a_2 + \beta_2 a_2 \sin\psi_3 + \beta_3 a_1 a_3 \sin\psi_2 = 0, \tag{29}$$

$$-\tfrac{1}{2}\hat{\sigma}_2 a_2 + \beta_2 a_2 \cos\psi_3 + \beta_3 a_1 a_3 \cos\psi_2 = 0, \tag{30}$$

$$\gamma_1 a_3 - \gamma_2 a_1 a_2 \sin\psi_2 = 0, \tag{31}$$

$$-\left[\tfrac{1}{2}(\hat{\sigma}_1 + \hat{\sigma}_2) - \sigma_1\right] a_3 + \gamma_2 a_1 a_2 \cos\psi_2 = 0. \tag{32}$$

There are two possible cases:

either $a_1 = a_2 = a_3 = 0$
or

$$a_1^2 = \frac{-\lambda_4 \pm \sqrt{\lambda_4^2 - 4\lambda_2\lambda_3}}{2\lambda_1\lambda_3}, \tag{33}$$

$$a_2^2 = \frac{-\lambda_7 \pm \sqrt{\lambda_7^2 - 4\lambda_5\lambda_6}}{2\lambda_1\lambda_6}, \tag{34}$$

$$a_3^2 = \frac{\left[-\lambda_4 \pm \sqrt{\lambda_4^2 - 4\lambda_2\lambda_3}\right]\left[-\lambda_7 \pm \sqrt{\lambda_7^2 - 4\lambda_5\lambda_6}\right]}{4\lambda_1\lambda_3\lambda_6}, \tag{35}$$

where $\lambda_1, \ldots, \lambda_7$ are given in the appendix.

From equation (33), it is concluded that:

(i) when $\lambda_4 > 0$ then a_1 has only one possible real root whenever

$$4\left(\beta_1^2 - \beta_2^2\right) + \hat{\sigma}_2^2 < 0; \tag{36}$$

(ii) when $\lambda_4 < 0$ there are two possibilities:

either a_1 has only one possible real root as

$$\left[2\beta_1\gamma_1 - \hat{\sigma}_2\left(\tfrac{1}{2}(\hat{\sigma}_1 + \hat{\sigma}_2) - \sigma_1\right)\right]^2 - \left[4\left(\beta_1^2 - \beta_2^2\right) + \hat{\sigma}_2^2\right]\left[\gamma_1^2 + \left(\tfrac{1}{2}(\hat{\sigma}_1 + \hat{\sigma}_2) - \sigma_1\right)^2\right] > 0, \tag{37}$$

or a_1 has two possible real roots as the following condition is satisfied:

$$0 < \left[4\left(\beta_1^2 - \beta_2^2\right) + \hat{\sigma}_2^2\right]\left[\gamma_1^2 + \left(\tfrac{1}{2}(\hat{\sigma}_1 + \hat{\sigma}_2) - \sigma_1\right)^2\right] < \left[2\beta_1\gamma_1 - \hat{\sigma}_2\left(\tfrac{1}{2}(\hat{\sigma}_1 + \hat{\sigma}_2) - \sigma_1\right)\right]^2. \tag{38}$$

Likewise, equation (34) shows that there are two possible cases for the amplitude a_2 of the second mode:

(i) when $\lambda_7 > 0$ there exist only one possible real root if we have

$$4\left(\alpha_1^2 - \alpha_2^2\right) + \hat{\sigma}_1^2 < 0; \tag{39}$$

(ii) when $\lambda_7 < 0$ we have two possible cases:

either a_2 possesses only one possible real root under the condition

$$\left[2\alpha_1\gamma_1 - \hat{\sigma}_1\left(\tfrac{1}{2}(\hat{\sigma}_1 + \hat{\sigma}_2) - \sigma_1\right)\right]^2 - \left[4\left(\alpha_1^2 - \alpha_2^2\right) + \hat{\sigma}_1^2\right]\left[\gamma_1^2 + \left(\tfrac{1}{2}(\hat{\sigma}_1 + \hat{\sigma}_2) - \sigma_1\right)^2\right] > 0, \tag{40}$$

or a_2 has two possible real roots if the following condition is satisfied:

$$0 < \left[4\left(\alpha_1^2 - \alpha_2^2\right) + \hat{\sigma}_1^2\right]\left[\gamma_1^2 + \left(\tfrac{1}{2}(\hat{\sigma}_1 + \hat{\sigma}_2) - \sigma_1\right)^2\right] < \left[2\alpha_1\gamma_1 - \hat{\sigma}_1\left(\tfrac{1}{2}(\hat{\sigma}_1 + \hat{\sigma}_2) - \sigma_1\right)\right]^2. \tag{41}$$

As for the amplitude a_3 of the third mode, we have concluded, based on equation (35), that there are four possible cases:

(i) when $\lambda_4 > 0$ and $\lambda_7 > 0$, the amplitude a_3 will possess only one possible real root such that conditions (36) and (39) are satisfied;

(ii) when $\lambda_4 > 0$ and $\lambda_7 < 0$, a_3 has only one real root when conditions (36) and (40) are satisfied, while it has two possible real roots as conditions (36) and (41) are satisfied;
(iii) when $\lambda_4 < 0$ and $\lambda_7 > 0$, equation (35) has one possible real root as conditions (37) and (39) are satisfied, while it has two possible real roots as conditions (38) and (39) are satisfied;
(iv) when $\lambda_4 < 0$ and $\lambda_7 < 0$, equation (35) admits only one real root whenever conditions (37) and (40) are satisfied, two real roots when either conditions (37) and (41) or (38) and (40) are satisfied, while it has four possible real roots as conditions (38) and (41) are satisfied.

3.2.1. Modified amplitudes equations. In order to demonstrate the stability criteria of the obtained steady-state solutions, it is convenient to make the following transformations for the unknown functions A_1, A_2, A_3:

$$A_1 = B_1 \mathrm{e}^{\frac{\mathrm{i}}{2}\hat{\sigma}_1 t_1}, \qquad A_2 = B_2 \mathrm{e}^{\frac{\mathrm{i}}{2}\hat{\sigma}_2 t_1}, \qquad A_3 = B_3 \mathrm{e}^{\mathrm{i}(\frac{1}{2}(\hat{\sigma}_1+\hat{\sigma}_2)-\sigma_1)t_1}. \tag{42}$$

Then equations (13)–(15) become the following amplitude equations:

$$\mathrm{i}\frac{\mathrm{d}B_1}{\mathrm{d}t_1} + \left(-\frac{1}{2}\hat{\sigma}_1 + \mathrm{i}\alpha_1\right) B_1 + \alpha_2 \bar{B}_1 + \alpha_3 \bar{B}_2 B_3 = 0, \tag{43}$$

$$\mathrm{i}\frac{\mathrm{d}B_2}{\mathrm{d}t_1} + \left(-\frac{1}{2}\hat{\sigma}_2 + \mathrm{i}\beta_1\right) B_2 + \beta_2 \bar{B}_2 + \beta_3 \bar{B}_1 B_3 = 0, \tag{44}$$

$$\mathrm{i}\frac{\mathrm{d}B_3}{\mathrm{d}t_1} + \left(\sigma_1 - \frac{1}{2}(\hat{\sigma}_1 + \hat{\sigma}_2) + \mathrm{i}\gamma_1\right) B_3 + \gamma_2 B_1 B_2 = 0. \tag{45}$$

It can be verified from (42) that the stable property of the system in terms of the amplitudes A_1, A_2, A_3 is equivalent to that of the amplitudes B_1, B_2, B_3. Dividing the unknown variables into real and imaginary parts ($B_j = p_j + \mathrm{i}q_j$), the amplitude equations (43)–(45) yield the following nonlinear system of ordinary differential equations:

$$\frac{\mathrm{d}p_1}{\mathrm{d}t_1} + \alpha_1 p_1 - \left(\frac{1}{2}\hat{\sigma}_1 + \alpha_2\right) q_1 + \alpha_3(p_2 q_3 - p_3 q_2) = 0, \tag{46}$$

$$\frac{\mathrm{d}q_1}{\mathrm{d}t_1} + \left(\frac{1}{2}\hat{\sigma}_1 - \alpha_2\right) p_1 + \alpha_1 q_1 - \alpha_3(p_2 p_3 + q_2 q_3) = 0, \tag{47}$$

$$\frac{\mathrm{d}p_2}{\mathrm{d}t_1} + \beta_1 p_2 - \left(\frac{1}{2}\hat{\sigma}_2 + \beta_2\right) q_2 + \beta_3(p_1 q_3 - p_3 q_1) = 0, \tag{48}$$

$$\frac{\mathrm{d}q_2}{\mathrm{d}t_1} + \left(\frac{1}{2}\hat{\sigma}_2 - \beta_2\right) p_2 + \beta_1 q_2 - \beta_3(p_1 p_3 + q_1 q_3) = 0, \tag{49}$$

$$\frac{\mathrm{d}p_3}{\mathrm{d}t_1} + \gamma_1 p_3 + \left(\sigma_1 - \frac{1}{2}(\hat{\sigma}_1 + \hat{\sigma}_2)\right) q_3 + \gamma_2(p_1 q_2 + p_2 q_1) = 0, \tag{50}$$

$$\frac{\mathrm{d}q_3}{\mathrm{d}t_1} - \left(\sigma_1 - \frac{1}{2}(\hat{\sigma}_1 + \hat{\sigma}_2)\right) p_3 + \gamma_1 q_3 - \gamma_2(p_1 p_2 - q_1 q_2) = 0. \tag{51}$$

The system of equations (46)–(51) can be rewritten in the following form,

$$\frac{\mathrm{d}\boldsymbol{\Theta}}{\mathrm{d}t_1} = \boldsymbol{\xi}(\boldsymbol{\Theta}), \tag{52}$$

where $\boldsymbol{\Theta} = (p_1, q_1, p_2, q_2, p_3, q_3)^T$ represents a column matrix (the transpose of the row matrix $(p_1, q_1, p_2, q_2, p_3, q_3)$) and $\boldsymbol{\xi}$ is a six-dimensional vector function of the variables p_j

and q_j. If $\boldsymbol{\Theta} = \boldsymbol{\Theta}_0$ represents a steady-state solution of equation (52), then we can check the linear stability of this solution by superimposing on it a disturbance a time-dependent vector function $\boldsymbol{\chi}(t_1)$ and hence we obtain the following perturbed equation:

$$\frac{\mathrm{d}\boldsymbol{\chi}}{\mathrm{d}t_1} = \boldsymbol{\xi}(\boldsymbol{\Theta}_0 + \boldsymbol{\chi}). \tag{53}$$

At this stage, we expand equation (53) about $\boldsymbol{\Theta}_0$ for a small $\boldsymbol{\chi}$, utilizing the relation $\boldsymbol{\xi}(\boldsymbol{\Theta}_0) = 0$, and retaining only the linear terms of $\boldsymbol{\chi}$, we have the linear variational equation

$$\frac{\mathrm{d}\boldsymbol{\chi}}{\mathrm{d}t_1} = (\nabla\boldsymbol{\xi}(\boldsymbol{\Theta}_0))\boldsymbol{\chi}. \tag{54}$$

Now, a steady-state solution $\boldsymbol{\Theta}_0$ for equation (52) will be asymptotically stable if the real parts of all the eigenvalues of the corresponding matrix $\nabla\boldsymbol{\xi}(\boldsymbol{\Theta}_0)$ (a matrix of dimension 6×6) are negative and otherwise, we have an unstable solution.

However, the eigenvalues ν of the system of equations (46)–(51) will be determined from the following equation:

$$\begin{vmatrix}
\nu+\alpha_1 & -\alpha_2-\frac{1}{2}\hat{\sigma}_1 & \alpha_3 q_3 & -\alpha_3 p_3 & -\alpha_3 q_2 & -\alpha_3 p_2 \\
-\alpha_2+\frac{1}{2}\hat{\sigma}_1 & \nu+\alpha_1 & -\alpha_3 p_3 & -\alpha_3 q_3 & -\alpha_3 p_2 & -\alpha_3 q_2 \\
\beta_3 q_3 & -\beta_3 p_3 & \nu+\beta_1 & -\beta_2-\frac{1}{2}\hat{\sigma}_2 & -\beta_3 q_1 & \beta_3 p_1 \\
-\beta_3 p_3 & -\beta_3 q_3 & -\beta_2+\frac{1}{2}\hat{\sigma}_2 & \nu+\beta_1 & -\beta_3 p_1 & -\beta_3 q_1 \\
\gamma_2 q_2 & \gamma_2 p_2 & \gamma_2 q_1 & \gamma_2 p_1 & \nu+\gamma_1 & -\frac{1}{2}(\hat{\sigma}_1+\hat{\sigma}_2)+\sigma_1 \\
-\gamma_2 p_2 & \gamma_2 q_2 & -\gamma_2 p_1 & \gamma_2 q_1 & \frac{1}{2}(\hat{\sigma}_1+\hat{\sigma}_2)-\sigma_1 & \nu+\gamma_1
\end{vmatrix} = 0,$$

or

$$F(\nu) = \nu^6 + b_5\nu^5 + b_4\nu^4 + b_3\nu^3 + b_2\nu^2 + b_1\nu + b_0 = 0. \tag{55}$$

The necessary and sufficient conditions for the real parts of all the roots of equation (55) to be non-positive—i.e. for the considered perturbation to be stable—are [31]

$$D_j > 0, \qquad j = 1, 2, \ldots, 6 \tag{56}$$

where the quantities D_j are given in the appendix.

To demonstrate the stability behavior of the trivial steady-state solution, we set $p_j = 0$, $q_j = 0$ in equation (55). Then we have the characteristic equation

$$F(\nu) = \nu^6 + \tilde{b}_5\nu^5 + \tilde{b}_4\nu^4 + \tilde{b}_3\nu^3 + \tilde{b}_2\nu^2 + \tilde{b}_1\nu + \tilde{b}_0 = 0, \tag{57}$$

where the coefficients $\tilde{b}_0, \tilde{b}_1, \tilde{b}_2, \ldots$ are given in the appendix.

4. Numerical applications

In this section, our main goal is to present a graphical illustration for the theoretical analysis that has been performed in this work. Firstly, the frequency–response curves corresponding to the possible steady-state solutions of the modulation equations are examined. We focus, of course, our attention on the positive real roots of the modified-amplitude solutions. However, the steady-state amplitudes a_n as well as the phases γ_n depend on the parameters: the two amplitudes f_1, f_2 of excitation, the detuning parameters $\sigma_1, \hat{\sigma}_1, \hat{\sigma}_2$, and the viscosity factor $\hat{\mu}_\ell$. Plots of the amplitudes a_n versus the detuning parameters $\hat{\sigma}_1$ and $\hat{\sigma}_2$ are presented in figures 1–3. The stability of the possible non-negative real fixed points is investigated via

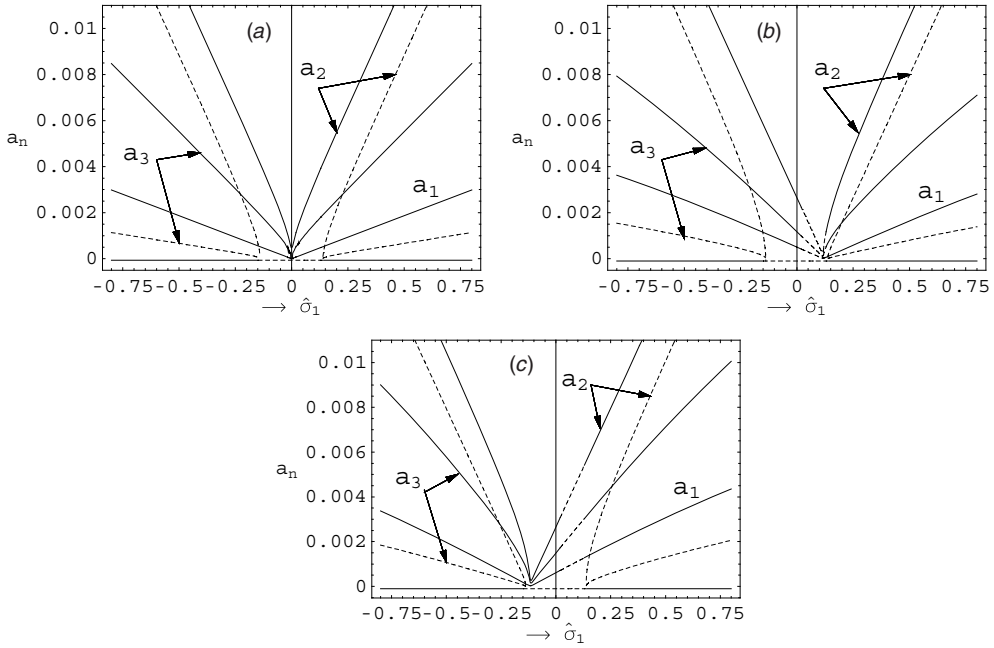

Figure 1. Frequency–response curves for the case $\omega_2 \simeq 2\omega_1$ and $\omega_2 \simeq 2\omega_1$, in the plane $a_n - \hat{\sigma}_1$, for a system having $M = 1.5$, $L = 1$, $\rho = 0.85$, $k_1 = 1.1$, $k_2 = 1.9$, $\epsilon = 0.05$, $\hat{\mu}_\ell = 0.05$, $f_1 = 10$, $f_2 = 19.4126$, $\hat{\sigma}_2 = 0$: (*a*) $\sigma_1 = 0$, (*b*) $\sigma_1 = 0.058$, (*c*) $\sigma_1 = -0.058$.

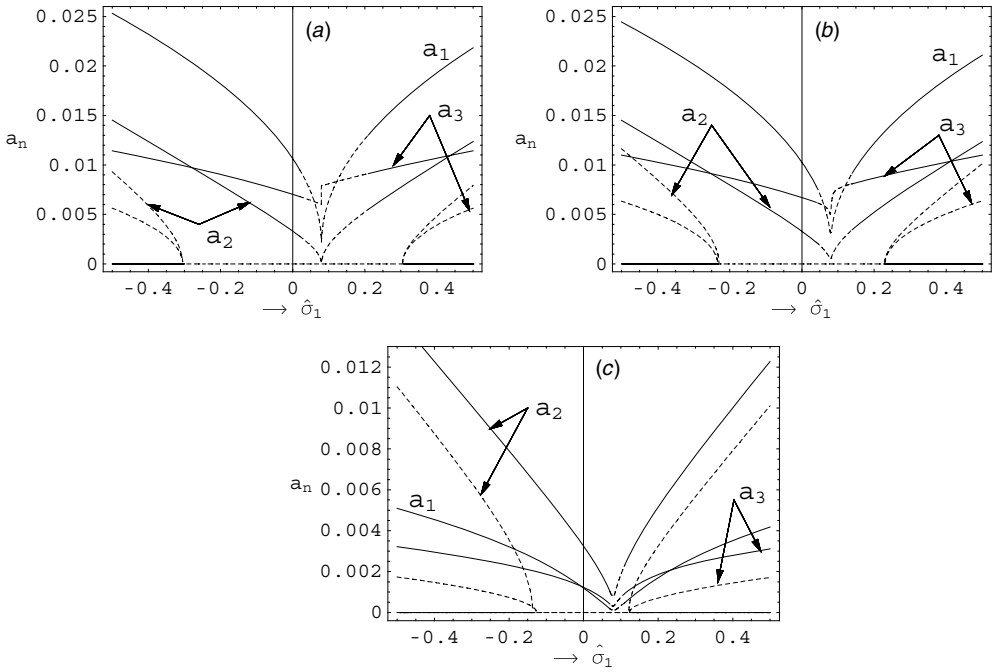

Figure 2. Frequency–response curves for the same case of resonance as in figure 1 in the plane $a_n - \hat{\sigma}_1$, for the same system considered in figure 1 but $f_1 = 20$, $f_2 = 21$, $\sigma_1 = 0.04$ and $\hat{\sigma}_2 = 0$: (*a*) $\hat{\mu}_\ell = 0$, (*b*) $\hat{\mu}_\ell = 0.02$, (*c*) $\hat{\mu}_\ell = 0.054$.

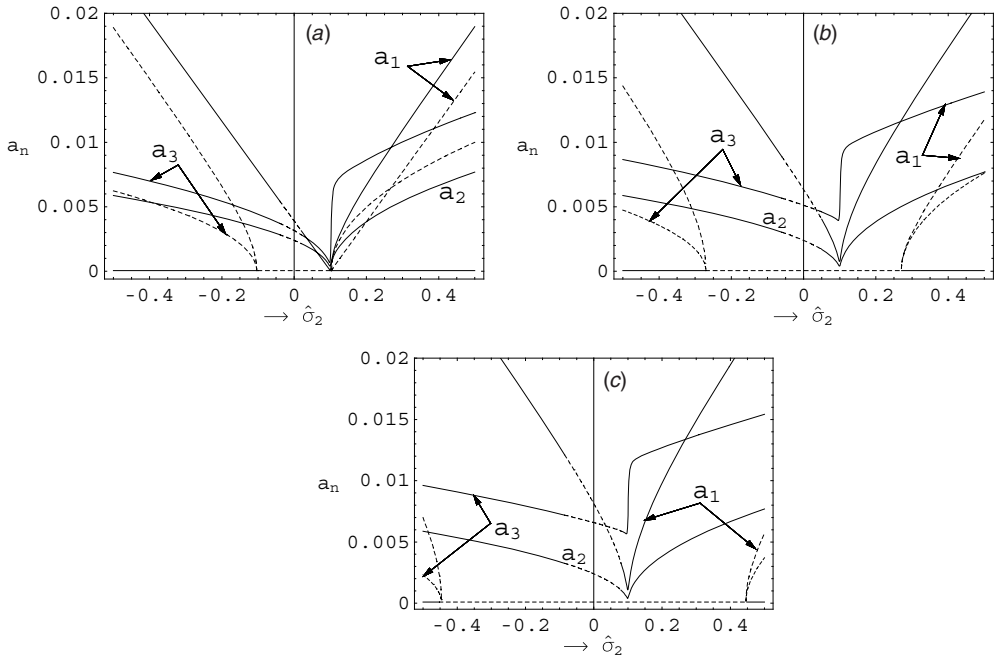

Figure 3. Variation of the steady-state solutions in the $a_n - \hat{\sigma}_2$ plane for the same system considered in figure 1, but $\hat{\mu}_\ell = 0.02$, $f_1 = 15$, $\hat{\sigma}_1 = 0$ and $\sigma_1 = 0.1$: (*a*) $f_2 = 12.9$, (*b*) $f_2 = 28$, (*c*) $f_2 = 45$.

examination of the stability conditions given by (56). Figure 1 represents the influence of the variation of the detuning parameter σ_1 on the frequency–response curves for the resonance case assigned by the relations $\omega_2 \simeq 2\omega_1$ and $\omega_2 \simeq 2\omega_1$, in the plane $a_n - \hat{\sigma}_1$. However, some variation of the parameter σ_1 has been successively considered for the sake of comparison in all parts of figure 1, with non-dimensional physical variables given by $M = 1.5, L = 1$, $\rho = 0.85, k_1 = 1.1, k_2 = 1.9, \epsilon = 0.05, \hat{\mu}_\ell = 0.05, f_1 = 10, f_2 = 19.4126, \hat{\sigma}_2 = 0$ and $\sigma_1 = 0$. As shown in figure 1(*a*), it is clear that when $\hat{\sigma} \leqslant -0.148$ or $\hat{\sigma}_1 \geqslant 0.148$, the modulational equations admit three possible steady-state solutions: the trivial solutions (the steady-solutions with initial zero modified amplitudes) which, in view of the stability conditions (56), is concluded to be stable (sink) and two nontrivial solutions (the steady-solution with at least nonzero initial modified amplitude). The first solution (the larger one) which is stable (sink), while the second (the smaller one) is unstable (saddle point). Thus the system response is either trivial or periodic. In other words, the resonant free surface waves either possess initially and subsequently zero modified amplitudes or they possess nonzero modified amplitudes that vary in a periodic manner. On the other hand, we observe that the lower fixed point has only two possible modes, the second and the third modes, while the modified amplitude that corresponds to the first mode (a_1) is not possible because of its being either negative or complex. When $-0.148 \leqslant \hat{\sigma}_1 \leqslant 0.148$, the system of the modulational equations admits two possible fixed points. The first one is the trivial solution which is unstable (saddle) and nontrivial solution (sink). It should be noted that both a_n and $-a_n$ represent solutions of the steady-state modified equations and thereby, in the light of the bifurcation theory, the system exhibits a subcritical pitchfork bifurcation at the values $\hat{\sigma}_1 = -0.148$ and 0.148. In this case, when $\hat{\sigma}_1$ increases past -0.148, the sink at the origin

becomes a saddle point and two saddles (corresponding to a_n and $-a_n$) will shrink towards the sink at the origin at $\hat{\sigma}_1 = -0.148$. In a similar manner, as $\hat{\sigma}_1$ decreases past the value 0.148, the sink at the origin turns to a saddle point at the value $\hat{\sigma}_1 = 0.148$. However, according to the bifurcation theorems, a bifurcation of the Hopf type would be expected to occur in the presence of such a symmetric property of system solutions. This result is in good agreement with those obtained by Miles [17]. The graphs displayed in figure 1(*b*) demonstrate the variation of the modified amplitudes of the steady-state solutions with the detuning parameter $\hat{\sigma}_1$ for the same system as considered in figure 1(*a*), but with $\sigma_1 = 0.058$. This figure shows that the positive value of σ_1 leads to shifting the frequency–response curves to right and moreover these curves lost its symmetry about the vertical axis. On the other hand, in view of the stability conditions (56), it is found that the trivial steady-state solution lacks such conditions throughout the specific interval satisfying the relation $0.02 \leqslant \hat{\sigma}_1 \leqslant 0.13$, while this solution is still stable throughout the same domain of σ_1 as determined in the case of the exact resonance ($\sigma_1 = 0$) studied in figure 1(*a*). Further, the characteristic equation (55) shows that within the interval $0.02 \leqslant \hat{\sigma}_1 \leqslant 0.13$, the nontrivial solution loses its stability with a pair of complex conjugate eigenvalues associated with positive real parts. In other words, when $\hat{\sigma}_1$ increases above 0.02 or decreases below 0.13, the nontrivial fixed point loses its stability, where the complex eigenvalues of the dispersion relation cross the imaginary axis into the right half of the complex plane. Consequently, the points $\hat{\sigma}_1 = 0.02, 0.13$ represent Hopf bifurcation ones for the investigated system. Thereby, based on the Hopf bifurcation theorems, two limit-cycle solutions of the evolution equations will be created near the points $\hat{\sigma}_1 = 0.02, 0.13$ where its sizes grow gradually from zero and proportional to $|\hat{\sigma}_1 - 0.02|^{\frac{1}{2}}$ and $|\hat{\sigma}_1 - 0.13|^{\frac{1}{2}}$, for $\hat{\sigma}_1$ closes to 0.02, 0.13, respectively. Figure 1(*c*) illustrates a picture of the system–response curves with the consistency of the model as in figure 1(*a*), but as $\sigma_1 = -0.058$. This portrait clearly shows that the behavior of the system response is very similar to that demonstrated in figure 1(*b*), but the system has lost its symmetry in this time via shifting the curves to lift.

The effect of changing the factor $\hat{\mu}_\ell$ on the qualitative response of modified amplitudes with the parameter $\hat{\sigma}_1$ is depicted in figures 2(*a*)–(*c*), for the same system considered in figure 1 but $f_1 = 20$, $f_2 = 21$, $\sigma_1 = 0.04$, $\hat{\sigma}_2 = 0$. In figure 2(*a*) the effect of the factor $\hat{\mu}_\ell$ is switched off, while in the remaining parts this effect is present where the values of $\hat{\mu}_\ell$ are increased to 0.02, 0.054, respectively. In part (*a*), we have remarked that as $\hat{\sigma}_1 \leqslant -0.303$, or $\hat{\sigma}_1 \geqslant 0.303$, we observe that the system has three possible steady-state solutions: the trivial solution, which is stable and two nontrivial solutions. Each of these solutions of course includes, in general, three possible modes. The first nontrivial solution (the larger one), which is stable, has three possible modes, whereas the second solution (the smaller one), which is unstable, has only the second and third modes while the first mode is not existent because of its being either negative or complex. In the intermediate region satisfying the relation $-0.303 \leqslant \hat{\sigma}_1 \leqslant 0.303$, it is found that the system has only two possible fixed points; each of them has three modes. The trivial solution is unstable (saddle), while the other solution is stable except for the specific range $0.02 \leqslant \hat{\sigma}_1 \leqslant 0.21$. Furthermore, the eigenvalue relation (55) shows that the nontrivial solution loses its stability via Hopf bifurcation at the points $\hat{\sigma}_1 = 0.02, 0.21$. This indicates that in the neighboring of the points $\hat{\sigma}_1 = 0.02$ and 0.21, the modulational equations admit aperiodic motions of the resonant waves. As the value of $\hat{\mu}_\ell$ is increased to 0.02, it is found that the trivial solution is unstable in the range $-0.233 \leqslant \hat{\sigma}_1 \leqslant 0.233$, and otherwise is stable. As for the lower nontrivial solution, it is existent and unstable in the regions $\hat{\sigma}_1 < -0.233$, and $\hat{\sigma}_1 > 0.233$, while the upper one loses its stability via Hopf bifurcation at the points $\hat{\sigma}_1 = 0.04$ and 0.14. Further increasing in the factor $\hat{\sigma}_1$ to the value 0.54 is considered in figure 2(*c*). This portrait shows that the unstable range of the trivial solution is contracted to $-0.133 \leqslant \hat{\sigma}_1 \leqslant 0.133$, while the unstable range of the nontrivial lower solution is enlarged to

$\hat{\sigma}_1 \leqslant -0.133$ and $\hat{\sigma}_1 \geqslant 0.133$. Hopf bifurcation has occurred at the points $\hat{\sigma}_1 = 0.07$ and 0.11. When the parts of figure 2 are compared with one another, we can conclude, broadly speaking, that the qualitative behavior of the stationary solutions of the modulational equations in the three cases are the same. Moreover, we conclude that the increasing in the viscosity factor enlarges the ranges of stability with respect to both the trivial solution as well as the upper nontrivial one, whereas it increases the region of instability with respect to the lower solution. This means that when the values of the viscosity factor are increased the Hopf bifurcation points move towards each other.

The aim of the graphs displayed in figures 3(*a*)–(*c*) is to justify the influence of the increase in the amplitude f_2 of the second mode of excitation on the frequency–response curves with the variation of the detuning parameter $\hat{\sigma}_2$, as a bifurcation variable. The same system of figure 1 is considered. The parameters used in plotting figure 3(*a*) are $\hat{\mu}_\ell = 0.02$, $f_1 = 15, \hat{\sigma}_1 = 0, \sigma_1 = 0.1$ and $f_2 = 12.9$. This figure elucidates that when $\hat{\sigma}_2 \leqslant -0.1$ or $\hat{\sigma}_2 \leqslant 0.1$, the system possesses three different stationary solutions: a trivial solution, which is stable, and two nontrivial solutions with the larger one being stable while the smaller solution being unstable. Moreover, we observe that the larger solution has three possible modes (corresponding to the three modes of the resonant waves), while the lower solution has only two possible modes: the first and the third modes where the second is not admissible being always corresponds to complex number. As $\hat{\sigma}_2$ increases past -0.1 or decreases below 0.1 the trivial solution loses its stability and the modulational equations possess only two possible stationary solutions. A search, in the light of the characteristic equation (55) together with the stability conditions (56), reveals that the nontrivial solution loses its stability at the points $\hat{\sigma}_2 = -0.04$ and 0.02, with corresponding complex conjugate eigenvalues having real positive real parts. Thus the system exhibits Hopf bifurcation at the points $\hat{\sigma}_2 = -0.04$ and 0.02. As the value of the amplitude f_2 is increased to 28 in figure 3(*a*), we conclude that the system undergoes a transcritical bifurcation at the points $\hat{\sigma}_2 = -0.271$ and 0.271, and the Hopf bifurcation has occurred at the points $\hat{\sigma}_2 = -0.06$, and 0.05. A further increasing in the parameter f_2 to the value 45, as illustrated in part 3(*c*), clearly shows that the system still undergoes the transcritical bifurcation at $\hat{\sigma}_2 = -0.446$ and 0.446, while exhibiting Hopfs bifurcation at $\hat{\sigma}_2 = -0.085$ and 0.08. When the parts of figure 3 compared with one another, we can conclude that there is a resemblance in the qualitative behavior of the system as the second mode of the amplitude excitation f_2 is increased. However, having noted the regions of stability and instability of the steady-state solutions, a great influence of the increase in the amplitude f_2 on the system response has been observed. It is noted that the continuous increase in δ_2 contracts the range of stability with respect to the trivial solution and makes the Hopf bifurcation points to move away from each other. On the other hand, this increase leads to the contraction of the existence region of the unstable lower fixed point solution. In order to be sufficiently clear and comprehensive and to provide enough information about the behavior of the system being investigated, phase portraits for the set of the autonomous modulational equations rather than the original evolution equations must be performed using computer simulations based on numerical techniques. In practical solutions, it is well to keep in mind that the fixed point solutions correspond to periodic motion for the interfacial waves, whereas limit-cycle solutions correspond to aperiodic motions of the free surface waves, and noting that limit cycles are inherently nonlinear phenomena, they cannot occur in linear systems.

The aim of the graphs displayed in figures 4 and 5 is to investigate the phase portrait in the $q_1 - p_1$ and $q_3 - p_3$ planes as well as the variation p_1, q_1, p_3 and q_3 with the evolution of time in the neighborhood of Hopf bifurcation that the system undergoes at the point $\hat{\sigma}_1 = 0.01$, and with non-dimensional variables: $M = 1.5, L = 1, \rho = 0.85, k_1 = 1.1, k_2 = 1.9$,

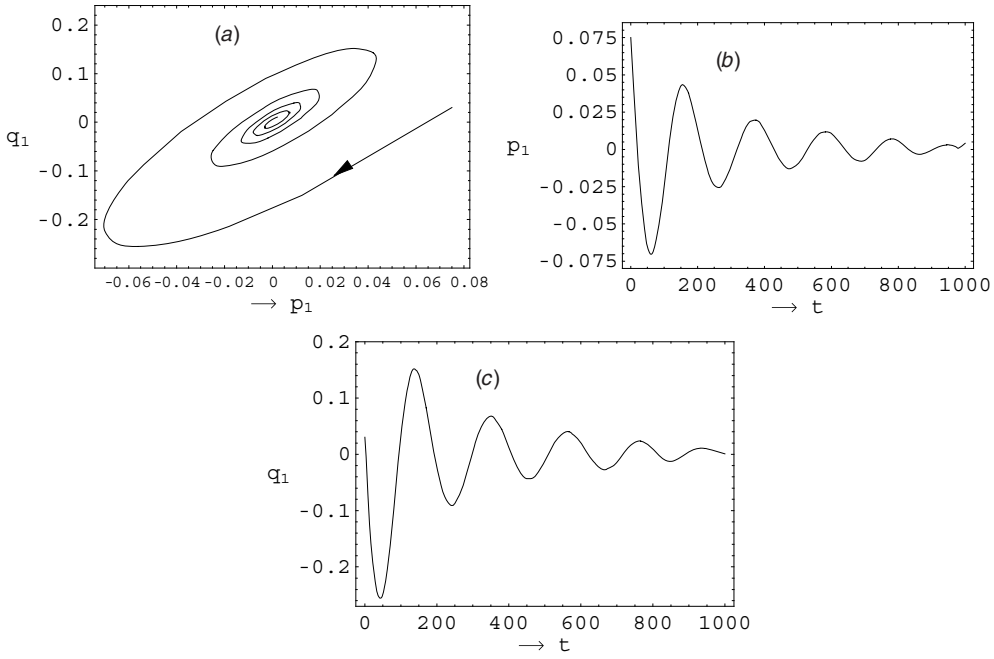

Figure 4. Projections of the trajectory of the modulation equations on the $q_1 - p_1$ plane as well as the variation of p_1, q_1 with the evolution of time at the value $\hat{\sigma}_1 = 0.01$, in the neighborhood of the Hopf bifurcation point at $\hat{\sigma}_1 = 0.02$, with the other parameters as in figure 1.

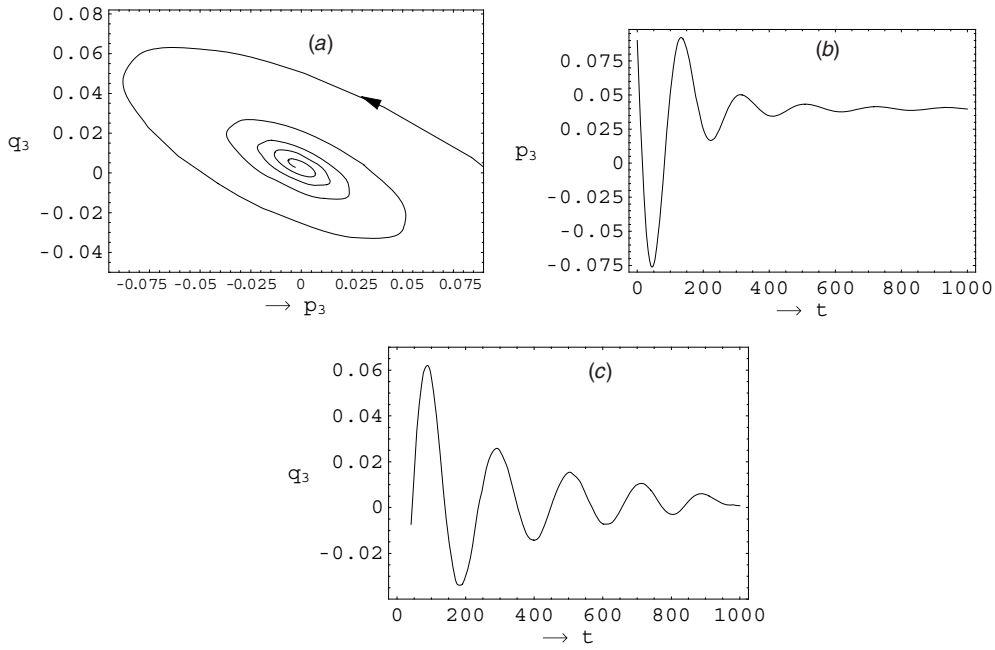

Figure 5. The same structure as in figure 4, but for p_3 and q_3.

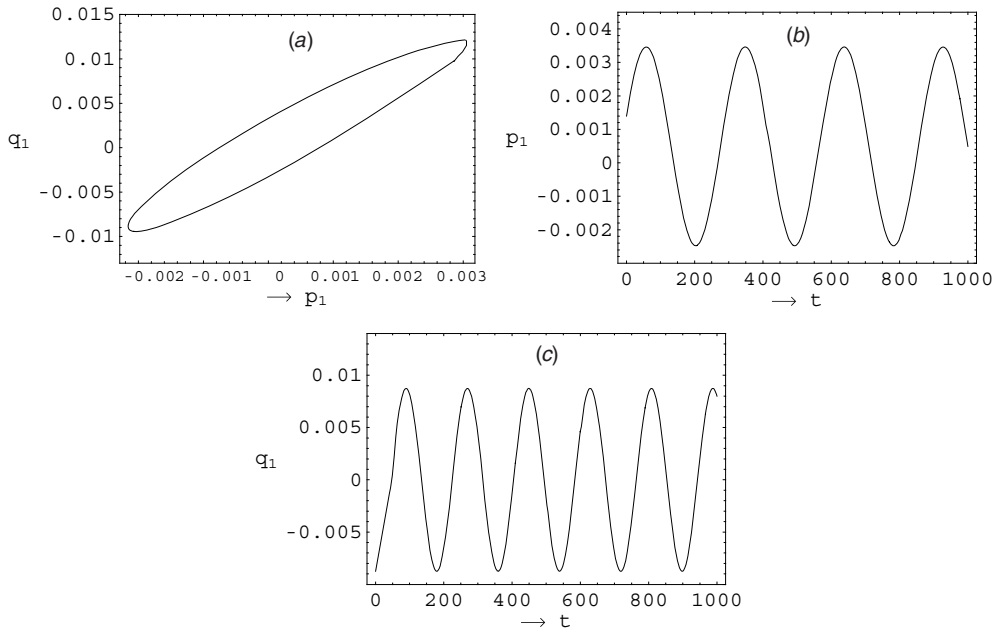

Figure 6. The same structure as in figure 4, but $\hat{\sigma}_1 = 0.02$.

$\epsilon = 0.05$, $\hat{\mu}_\ell = 0.05$, $f_1 = 10$, $f_2 = 19.4126$, and $\hat{\sigma}_2 = 0$. Figure 4(a) illustrates the phase portrait in the $q_1 - p_1$ plane, which represents a stable spiral that spirals with sense of clockwise rotation towards the limit cycle. On the other hand, figures 4(b), (c) clearly show the continuous decay of both of p_1 and q_1 with the development of time. On the other hand, we observe that the variation of each of p_1 and q_1 is very rapidly for the relatively small values of time, while it is very slower for large values of time. Figure 5 illustrates the phase portrait in the $q_3 - p_3$ plane as well as the behavior of p_3 and q_3 with the evolution of time. It is observed that the qualitative behavior of the system in both cases is very similar. However, the direction of spiraling in the two cases is opposite to each other. The phase portraits in the planes $q_1 - p_1$ and $q_3 - p_3$ at the Hobf bifurcation point $\hat{\sigma}_1 = 0.02$ are demonstrated in figures 6(a), 7(a), while figures 6(a), (b) and 7(a), (b) show the records of the corresponding variations in the modified amplitudes p_1, q_1, p_3 and q_3. It is observed that the limit cycle has an elliptical form in the $q_1 - p_1$ plane, while it has an oval form in the $q_3 - p_3$ plane. Further, we note that the solutions of the variable p_1, q_1, p_3 and q_3 settle down to be very similar to that of a sinusoidal oscillation of constant amplitudes, but with short time periods in the case of p_3 and q_3. Figures 8 and 9 show the computer-generated phase portraits as well as the solutions of the modulation equations as functions of time for the same values of the physical parameters as in figures 6 and 7, except that, the detuning parameter $\hat{\sigma}_1$ value is increased to 0.04 in the neighborhood of the limit cycle. These graphs clearly show that the trajectories in the neighborhood of the limit cycle represent unstable spirals that spiral towards this cycle and the solutions gradually grow with time. The inspection of the diagrams depicted in figures 4–9 then reveals that in the neighboring of the Hopf bifurcation point $\hat{\sigma}_1 = 0.02$ (below or above), the trajectories spiral asymptotically towards the limit cycle and thereby this cycle is of a stable kind or attracting. In view of the bifurcation theorems, it follows that the point $\hat{\sigma}_1 = 0.02$ represents a supercritical Hopf bifurcation. Stable limit cycles are very important scientifically—they model systems that exhibit self-sustained oscillations. In other words,

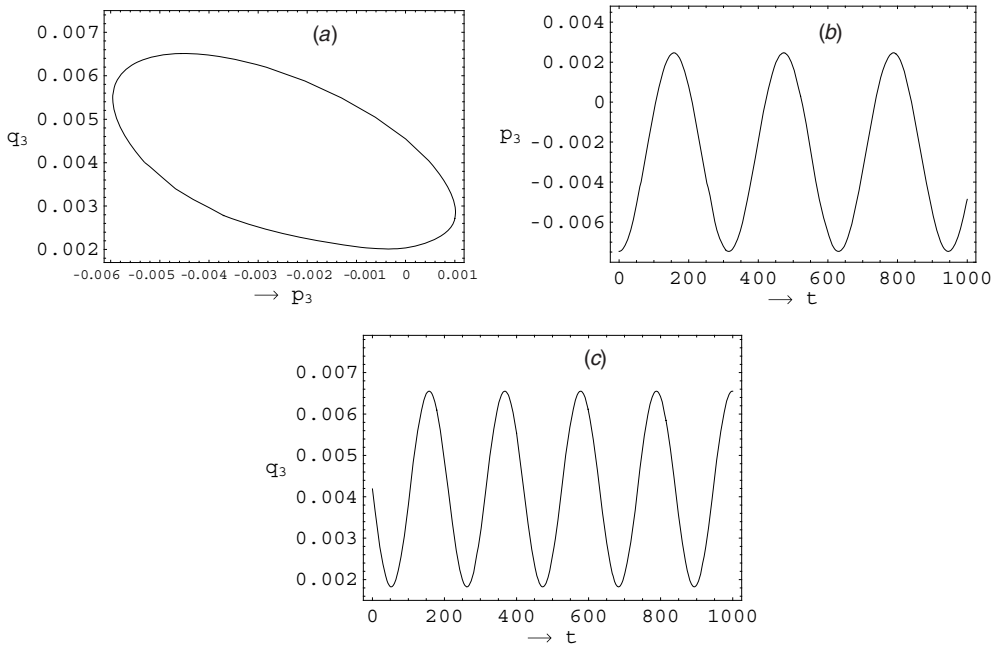

Figure 7. The same structure as in figure 5, but $\hat{\sigma}_1 = 0.02$.

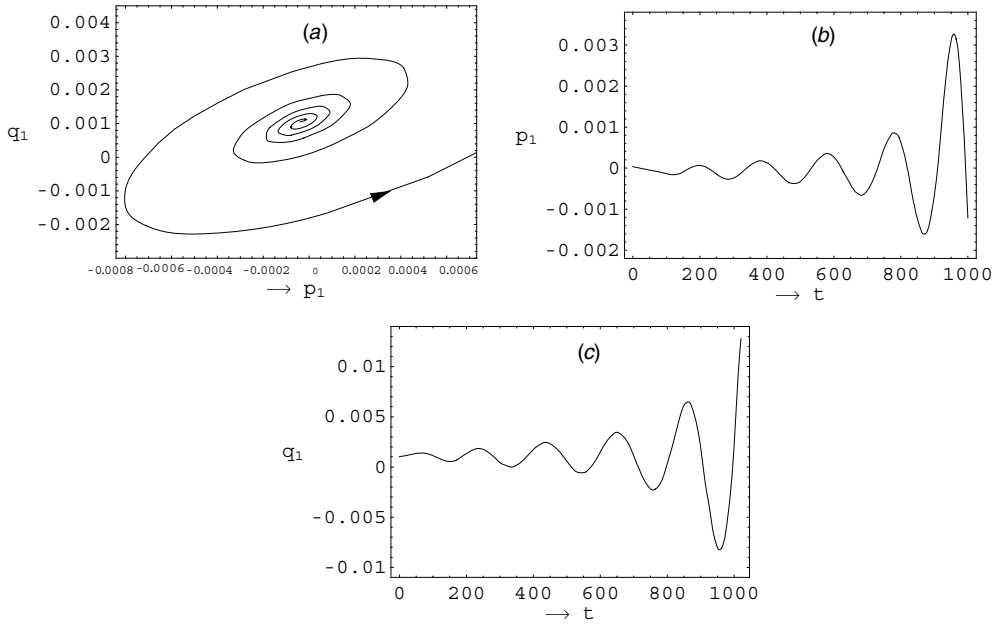

Figure 8. The same structure as in figure 4, but $\hat{\sigma}_1 = 0.04$.

these systems oscillate even in the absence of external periodic forcing. It is expected that as $\hat{\sigma}_1$ is increased over the values 0.04 that limit cycles, for instance in the planes $q_1 - p_1$ and $q_3 - p_3$,

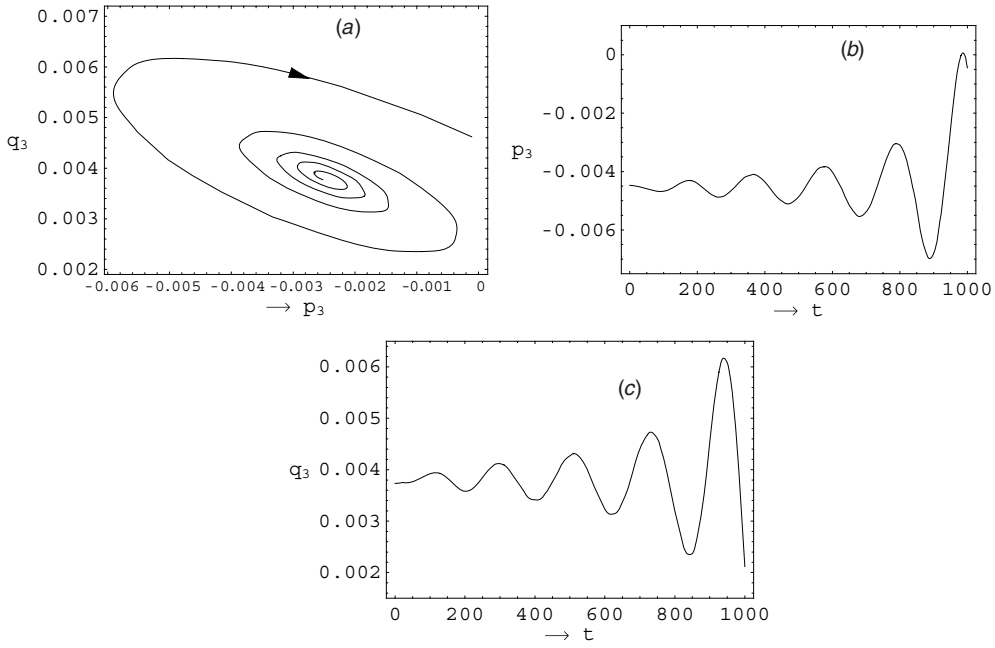

Figure 9. The same structure as in figure 5, but $\hat{\sigma}_1 = 0.04$.

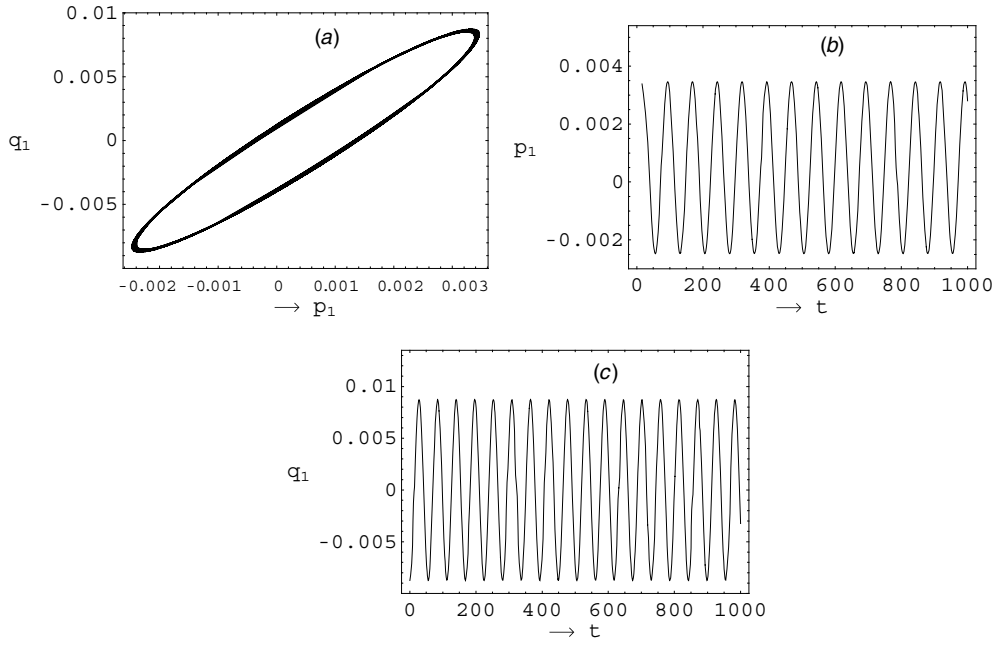

Figure 10. The phase portraits of the modulation equations as in figure 4, but $\hat{\sigma}_1$ has been increased to 0.072.

will have a period doubling, period quadrupling, ... etc. In figures 10 and 11, where $\hat{\sigma}_1$ possesses the value 0.072, we have two limit cycles that around themselves many times (many

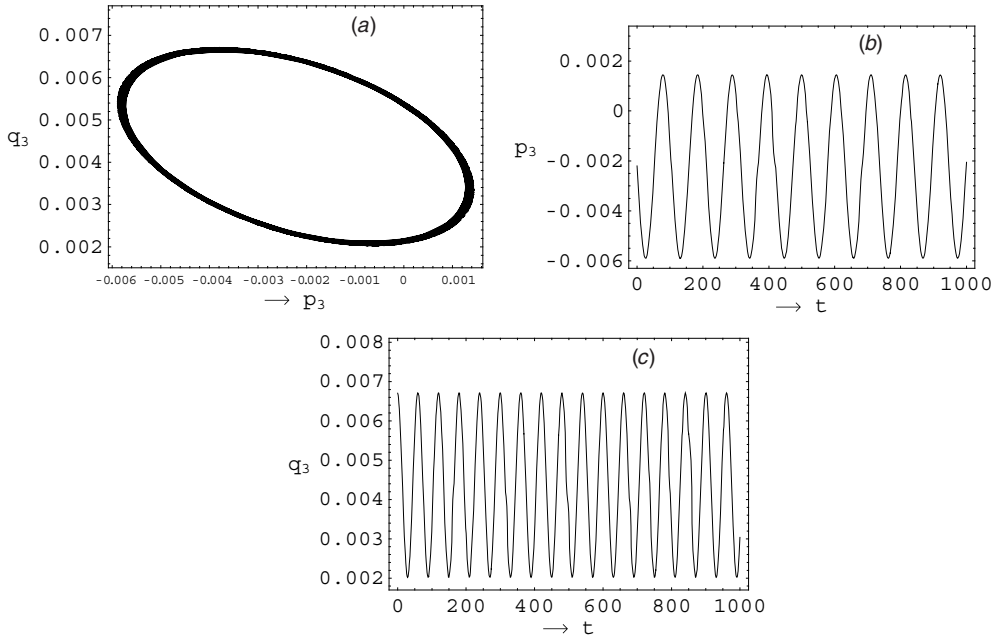

Figure 11. The same structure as in figure 10, but for p_3 and q_3.

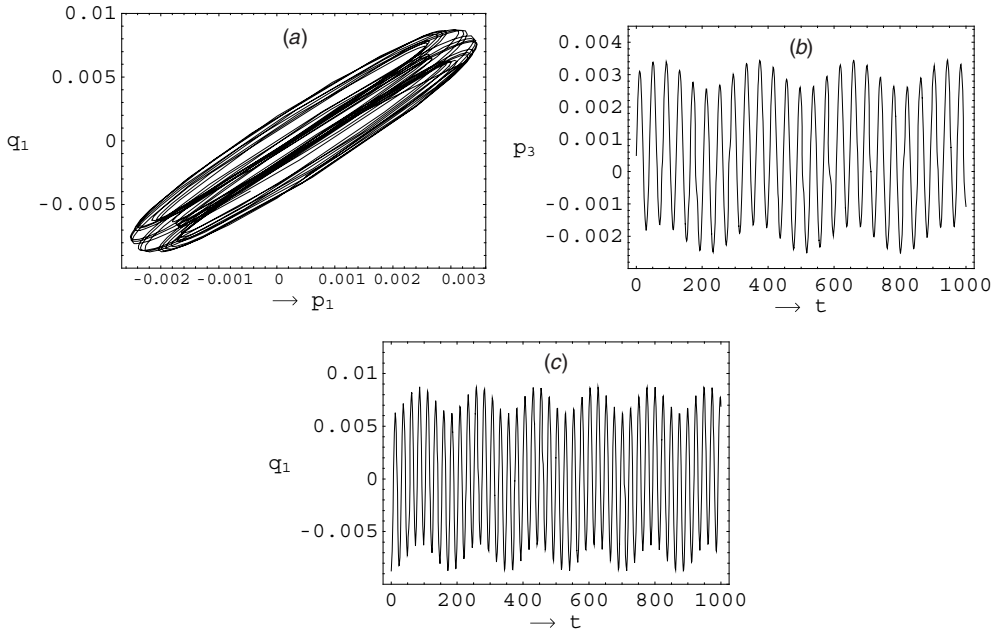

Figure 12. Projections of the modulation equations as in figure 4 but at $\hat{\sigma}_1 = 0.1$.

period doubling). However, after an infinite cascade of further period doubling, we obtain the strange attractor (the transition to chaotic motion) at the $\hat{\sigma}_1 = 0.1$, as shown in figures 12 and 13.

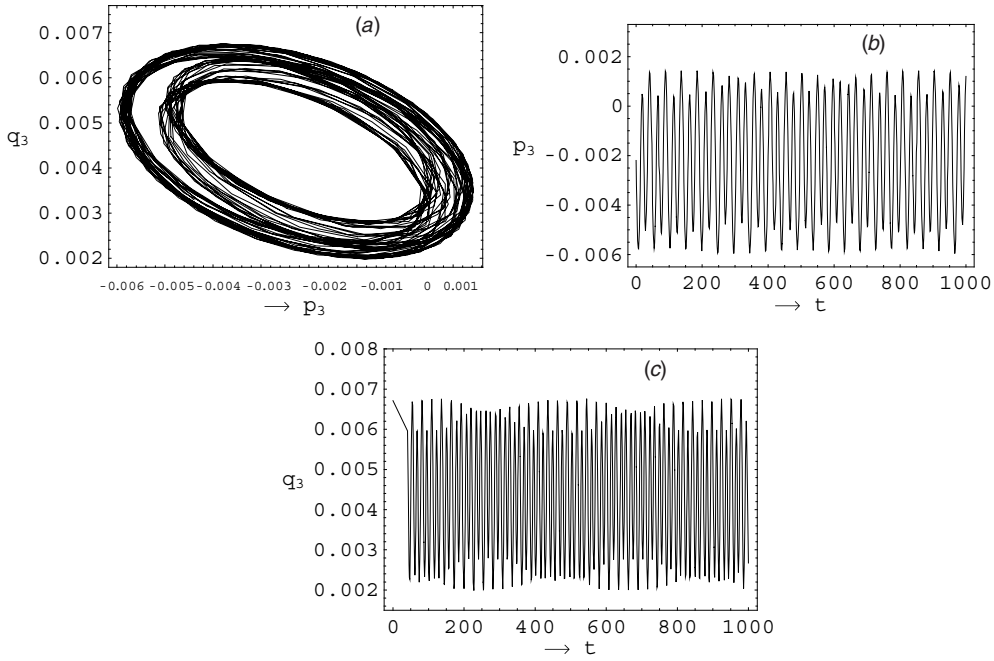

Figure 13. The same structure of figure 12 but for p_3 and q_3.

5. Conclusions

This work considers two semi-infinite layers of incompressible fluids in a rectangular container. The considered problem studies the resonant waves of three modes on the interface between fluids acted on by a periodic excitation along the direction normal to the liquid–liquid interface. The longitudinally exciting acceleration is assumed to decompose into two different frequencies. Using the method of multiple timescales, a system of nonlinear autonomous six-order ordinary differential equations governing the modulation of the amplitudes and phases of the resonant waves is obtained which is, in turn, exploited for determining the steady-state solutions and hence their stability. Conditions of existence of both regular periodic and chaotic regimes are obtained.

The numerical computations based on the modulational equations are achieved in order to investigate the evolutions of modified amplitudes with the development of time as well as the phase-plane trajectory. According to the theoretical analysis together with the numerical computations, we can conclude the following:

- The frequency response of the steady-state solutions, with the detuning parameter $\hat{\sigma}_1$ as a control one, the system response is either trivial or periodic and these curves exhibit only the pitchfork bifurcation at the exact resonance case.
- In the non-exact resonance case, the symmetry of the solution has been broken and a Hopf bifurcation type is created. This elucidates that the initial choice of $\hat{\sigma}_1$ has an important role in determining the qualitative behavior of the stationary solutions.
- The increase of the viscosity factor $\hat{\mu}_\ell$ has a regular stabilizing effect. Further, it moves the two created Hopf bifurcations towards each other.

- The increase in the values of the exciting amplitudes contacts the regions of the stable steady-state solutions and moreover it causes the Hopf bifurcations to move away from each other.
- As the values of the control parameter $\hat{\sigma}_1$ increase past the Hopf bifurcation point, the limit cycle goes more around itself before the transition to the case of the strange attractor.

Appendix

$$\alpha_1 = \frac{k_1^2\hat{\mu}_\ell}{1+\rho}, \qquad \alpha_2 = \frac{(1-\rho)k_1\delta_1}{4(1+\rho)\omega_1},$$

$$\alpha_3 = \frac{1}{4M^2N^2k_2k_3(1+\rho)\omega_1}\big[-2MN(\omega_2-\omega_3)(k_3(1-\rho)Q_3\omega_2 - k_2(1-\rho)Q_4\omega_3) - (1-\rho)k_1\big(-6(N^2+M^2)\pi^2\omega_2\omega_3 + N^2M^2k_2k_3\big(\omega_2^2+\omega_3^2\big)\big)\big],$$

$$\alpha_4 = \frac{1}{4M^2N^2k_2k_3(1+\rho)\omega_1}\big[-2MN(\omega_2+\omega_3)(k_3(1-\rho)Q_3\omega_2 + k_2(1-\rho)Q_4\omega_3) - (1-\rho)k_1\big(6(N^2+M^2)\pi^2\omega_2\omega_3 + N^2M^2k_2k_3\big(\omega_2^2+\omega_3^2\big)\big)\big],$$

$$\beta_1 = \frac{k_2^2\hat{\mu}_\ell}{1+\rho}, \qquad \beta_2 = \frac{(1-\rho)k_2\delta_2}{4(1+\rho)\omega_2},$$

$$\beta_3 = \frac{1}{-4M^2N^2k_1k_3(1+\rho)\omega_2}\big[2MN(\omega_1-\omega_3)(k_3(1-\rho)Q_6\omega_1 - k_1(1-\rho)Q_7\omega_3) + (1-\rho)k_2\big(-3(N^2+M^2)\pi^2\omega_1\omega_3 + N^2M^2k_1k_3\big(\omega_1^2+\omega_3^3\big)\big)\big],$$

$$\beta_4 = \frac{(1-\rho)k_2\delta_1}{4(1+\rho)\omega_2}, \qquad \gamma_1 = \frac{k_3^2\hat{\mu}_\ell}{1+\rho},$$

$$\gamma_2 = \frac{1}{-4M^2N^2k_1k_3(1+\rho)\omega_2}\big[2MN(\omega_1+\omega_2)(k_2(1-\rho)Q_8\omega_1 + k_1(1-\rho)Q_9\omega_2) + (1-\rho)k_3\big(-2(N^2+M^2)\pi^2\omega_1\omega_2 + N^2M^2k_1k_2\big(\omega_1^2+\omega_2^2\big)\big)\big],$$

$$\gamma_3 = \frac{(1-\rho)k_3\delta_2}{4(1+\rho)\omega_3},$$

$$\gamma_4 = \frac{1}{-4M^2N^2k_1k_2(1+\rho)\omega_3}\big[2\omega_2(\pi^2(M^2+N^2)(1-\rho)k_3\omega_1 + NMk_1Q_9(1-\rho)(\epsilon\sigma_2-\omega_3)) + NMk_2\big(NM(1-\rho)k_1k_3\big(\omega_1^2+\omega_2^2\big) + 2\rho\omega_1Q_8(\epsilon\sigma_2-\omega_3) + 2Q_8\omega_1(-\epsilon\sigma_2+\omega_3)\big)\big],$$

$$Q_{1,2} = \frac{\pi^2(M^2+N^2)}{MN} - \frac{1}{2}MNk_{1,2}^2, \qquad Q_{3,4} = \frac{3\pi^2(M^2+N^2)}{MN} - \frac{1}{2}MNk_{3,4}^2,$$

$$Q_5 = -\frac{\pi^2(M^2+N^2)}{2MN} - \frac{1}{2}MNk_1^2, \qquad Q_{6,7} = \frac{3\pi^2(M^2+N^2)}{2MN} - \frac{1}{2}MNk_{1,3}^2,$$

$$Q_{8,9} = -\frac{3\pi^2(M^2+N^2)}{MN} - \frac{1}{2}MNk_{1,2}^2.$$

$$\lambda_1 = \frac{\gamma_2^2}{\gamma_1^2 + \left[\frac{1}{2}(\hat{\sigma}_1+\hat{\sigma}_2) - \sigma_1\right]^2}, \qquad \lambda_2 = \left(\beta_1^2 - \beta_2^2 + \frac{1}{4}\hat{\sigma}_2^2\right)\gamma_2^2,$$

$$\lambda_3 = \beta_3^2\left[\gamma_1^2 + \left(\tfrac{1}{2}(\hat{\sigma}_1 + \hat{\sigma}_2) - \sigma_1\right)^2\right], \qquad \lambda_4 = 2\beta_1\beta_3\gamma_1\gamma_2 - \hat{\sigma}_2\beta_3\gamma_2\left[\tfrac{1}{2}(\hat{\sigma}_1 + \hat{\sigma}_2) - \sigma_1\right],$$

$$\lambda_5 = \gamma_2^2\left(\alpha_1^2 - \alpha_2^2 + \tfrac{1}{4}\hat{\sigma}_1^2\right), \qquad \lambda_6 = \alpha_3^2\left[\gamma_1^2 + \left(\tfrac{1}{2}(\hat{\sigma}_1 + \hat{\sigma}_2) - \sigma_1\right)^2\right],$$

$$\lambda_7 = 2\alpha_1\alpha_3\gamma_1\gamma_2 - \hat{\sigma}_1\alpha_3\gamma_2\left[\tfrac{1}{2}(\hat{\sigma}_1 + \hat{\sigma}_2) - \sigma_1\right].$$

$$D_1 = b_1, \qquad D_2 = \begin{vmatrix} b_1 & b_0 \\ b_3 & b_2 \end{vmatrix}, \qquad D_3 = \begin{vmatrix} b_1 & b_0 & 0 \\ b_3 & b_2 & b_1 \\ b_5 & b_4 & b_3 \end{vmatrix}, \qquad D_4 = \begin{vmatrix} b_1 & b_0 & 0 & 0 \\ b_3 & b_2 & b_1 & b_0 \\ b_5 & b_4 & b_3 & b_2 \\ 0 & 1 & b_5 & b_4 \end{vmatrix},$$

$$D_5 = \begin{vmatrix} b_1 & b_0 & 0 & 0 & 0 \\ b_3 & b_2 & b_1 & b_0 & 0 \\ b_5 & b_4 & b_3 & b_2 & b_1 \\ 0 & 1 & b_5 & b_4 & b_3 \\ 0 & 0 & 0 & 1 & b_5 \end{vmatrix}, \qquad D_6 = \begin{vmatrix} b_1 & b_0 & 0 & 0 & 0 & 0 \\ b_3 & b_2 & b_1 & b_0 & 0 & 0 \\ b_5 & b_4 & b_3 & b_2 & b_1 & b_0 \\ 0 & 1 & b_5 & b_4 & b_3 & b_2 \\ 0 & 0 & 0 & 1 & b_5 & b_4 \\ 0 & 0 & 0 & 0 & 0 & 1 \end{vmatrix}.$$

$$\begin{aligned}\tilde{b}_0 = {} & \tfrac{1}{4}\left(\alpha_1^2 - \alpha_2^2\right)\left[\gamma_1^2 + (\sigma_1 - \hat{\sigma}_1)\sigma_1 + \left(\tfrac{1}{2}\hat{\sigma}_1 - \sigma_1\right)\hat{\sigma}_2\right]\hat{\sigma}_2^2 \\ & + \tfrac{1}{16}\left(\alpha_1^2 - \alpha_2^2 + \gamma_1^2 + \sigma_1(\sigma_1 - \hat{\sigma}_1) + \tfrac{1}{64}\hat{\sigma}_1^4\right)\hat{\sigma}_1^2\hat{\sigma}_2^2 + \tfrac{1}{16}(2\hat{\sigma}_1 - \sigma_1)\hat{\sigma}_1^2\hat{\sigma}_2^3 \\ & + \tfrac{1}{16}\left(\alpha_1^2 - \alpha_2^2 + \tfrac{1}{4}\hat{\sigma}_1^2\right)\hat{\sigma}_2^4 + \left(\beta_2^2 - \beta_1^2\right)\left[\tfrac{1}{4}\left(\alpha_2^2 - \alpha_1^2\right)(2\hat{\sigma}_1 + \hat{\sigma}_2)\hat{\sigma}_2\right. \\ & \left. - \tfrac{1}{16}(2\hat{\sigma}_1 + \hat{\sigma}_2)\hat{\sigma}_1^2\hat{\sigma}_2 + \left(\alpha_2^2 - \alpha_1^2 - \tfrac{1}{4}\hat{\sigma}_1^2\right)\left(\gamma_1^2 + \sigma_1^2 - \sigma_1(\hat{\sigma}_1 + \hat{\sigma}_2) + \tfrac{1}{4}\hat{\sigma}_1^2\right)\right],\end{aligned}$$

$$\begin{aligned}\tilde{b}_1 = {} & \tfrac{1}{2}\left(\alpha_1^2 - \alpha_2^2\right)\gamma_1\hat{\sigma}_2^2 + \tfrac{1}{2}\alpha_1\left(\gamma_1^2 + \sigma_1^2\right)\hat{\sigma}_2^2 - \tfrac{1}{2}\alpha_1\sigma_1\hat{\sigma}_1\hat{\sigma}_2^2 + \tfrac{1}{8}(\alpha_1 + \gamma_1)\hat{\sigma}_2^2\hat{\sigma}_2^2 - \tfrac{1}{2}\alpha_1\sigma_1\hat{\sigma}_2^3 \\ & + \tfrac{1}{4}\alpha_1\hat{\sigma}_1\hat{\sigma}_2^3 + \tfrac{1}{8}\alpha_1\hat{\sigma}_2^4 + \left(\beta_1^2 - \beta_2^2\right)\left(2\alpha_1\gamma_1^2 + \gamma_1\left(2\alpha_1^2 - 2\alpha_2^2 + \tfrac{1}{2}\hat{\sigma}_1^2\right)\right. \\ & \left. + \alpha_1\left(2\sigma_1^2 + 0.5(\hat{\sigma}_1 + \hat{\sigma}_2)^2 - 2\sigma_1(\hat{\sigma}_1 + \hat{\sigma}_1)\right)\right) \\ & + \beta_1\left(\alpha_1^2 - \alpha_2^2 + \tfrac{1}{4}\hat{\sigma}_1^2\right)\left(2\left(\gamma_1^2 + \sigma_1^2\right) + (\hat{\sigma}_1 + \hat{\sigma}_2)(\hat{\sigma}_1 + \hat{\sigma}_2 - 2\sigma_1)\right),\end{aligned}$$

$$\begin{aligned}\tilde{b}_2 = {} & \left(\gamma_1^2 + \sigma_1^2\right)\left(\alpha_1^2 - \alpha_2^2 + \tfrac{1}{4}\left(\hat{\sigma}_1^2 + \hat{\sigma}_2^2\right)\right) + \left(\alpha_1^2 - \alpha_2^2\right)\left(-\sigma_1\hat{\sigma}_1 + \tfrac{1}{4}\hat{\sigma}_1^2 + \tfrac{1}{2}\hat{\sigma}_1\hat{\sigma}_2 + \tfrac{1}{2}\hat{\sigma}_2^2\right) \\ & - \tfrac{1}{4}\sigma_1\hat{\sigma}_1^3 + \tfrac{1}{16}\hat{\sigma}_1^4 - \tfrac{1}{4}\sigma_1\sigma_2\hat{\sigma}_1^2 + \tfrac{1}{8}\hat{\sigma}_1^3\hat{\sigma}_2 + \alpha_1\gamma_1\hat{\sigma}_2^2 - \tfrac{1}{4}\sigma_1\hat{\sigma}_1\hat{\sigma}_2^2 + \tfrac{3}{16}\hat{\sigma}_1^2\hat{\sigma}_2^2 \\ & - \tfrac{1}{4}\sigma_1\hat{\sigma}_2^3 + \tfrac{1}{8}\hat{\sigma}_1\hat{\sigma}_2^3 + \tfrac{1}{16}\hat{\sigma}_2^4 + \left(\beta_1^2 - \beta_2^2\right)\left(\alpha_1^2 - \alpha_1^2 + 4\alpha_1\gamma_1 + \gamma_1^2 + \sigma_1^2\right. \\ & \left. + \tfrac{1}{2}\hat{\sigma}_1^2 + \tfrac{1}{2}\hat{\sigma}_1\hat{\sigma}_2 + \tfrac{1}{4}\hat{\sigma}_2^2 - \sigma_1(\hat{\sigma}_1 + \hat{\sigma}_2)\right) + \beta_1\left(4\alpha_1\gamma_1^2 + \gamma_1\left(4\alpha_1^2 - 4\alpha_2^2 + \hat{\sigma}_1^2\right)\right. \\ & \left. + \alpha_1(-\sigma_1 + \hat{\sigma}_1 + \hat{\sigma}_2)^2\right),\end{aligned}$$

$$\begin{aligned}\tilde{b}_3 = {} & 2\left(\alpha_1^2 - \alpha_2^2\right)\gamma_1 + 2\left(\beta_1^2 - \beta_2^2\right)(\alpha_1 + \gamma_1) + 2\alpha_1\left(\gamma_1^2 + \sigma_1^2\right) + \tfrac{1}{2}(\alpha_1 + \gamma_1)\hat{\sigma}_1^2 + \alpha_1\hat{\sigma}_1\hat{\sigma}_2 \\ & + \left(\alpha_1 + \tfrac{1}{2}\gamma_1\right)\hat{\sigma}_2^2 - 2\alpha_1\sigma_1(\hat{\sigma}_1 + \hat{\sigma}_2) + \beta_1\left(2\alpha_1^2 - 2\alpha_2^2 + 8\alpha_1\gamma_1 + 2\gamma_1^2 + 2\sigma_1^2\right. \\ & \left. + \hat{\sigma}_1^2 + \hat{\sigma}_1\hat{\sigma}_2 + \tfrac{1}{2}\hat{\sigma}_2^2 - 2\sigma_1(\hat{\sigma}_1 + \hat{\sigma}_2)\right),\end{aligned}$$

$$\begin{aligned}\tilde{b}_4 = {} & \alpha_1^2 - \alpha_2^2 + \beta_1^2 - \beta_2^2 + 4\alpha_1\gamma_1 + \gamma_1^2 + 4\beta_1(\alpha_1 + \gamma_1) + \sigma_1^2 - \sigma_1\hat{\sigma}_1 + \tfrac{1}{2}\hat{\sigma}_1^2 \\ & + \left(-\sigma_1 + \tfrac{1}{2}(\hat{\sigma}_1 + \hat{\sigma}_2)\right)\hat{\sigma}_2,\end{aligned}$$

$$\tilde{b}_5 = 2(\alpha_1 + \beta_1 + \gamma_1).$$

References

[1] Faraday M 1831 On a peculiar class of acoustical figures; and on certain forms assumed by groups of particles upon vibrating elastic surfaces *Phil. Trans. R. Soc. Lond.* **121** 299–340

[2] Benjamin T B and Ursell F 1954 The stability of the plane free surface of a liquid in vertical periodic motion *Proc. R. Soc. Lond.* A **225** 505–15
[3] Miles J 1984 Nonlinear Faraday resonance *J. Fluid Mech.* **146** 285–302
[4] Gu X M, Sethna P R and Narain A 1988 On three-dimensional nonlinear subharmonic resonant surface waves in a fluid: I. Theory *J. Appl. Mech.* **55** 213–9
[5] Miles J 1993 On Faraday waves *J. Fluid Mech.* **248** 671–83
[6] Miles J 1999 On Faraday resonance of a viscous liquid *J. Fluid Mech.* **395** 321–5
[7] Mancebo F and Vega J 2002 Faraday instability threshold in large-aspect-ratio containers *J. Fluid Mech.* **467** 307–30
[8] Westra M, Binks D and Van de Water W 2003 Patterns of Faraday waves *J. Fluid Mech.* **496** 1–32
[9] Liu X, Wang D and Chen Y 1995 Self-excited vibration of the shell-liquid coupled system induced by dry friction *Acta Mech. Sin.* **11** 373–82
[10] Sun S M, Shen M C and Hsieh D Y 1995 Nonlinear theory of forced surface waves in a circular basin *Wave Motion* **21** 331–41
[11] Shen M C, Sun S M and Hsieh D Y 1993 Forced capillary-gravity waves in a circular basin *Wave Motion* **18** 401–12
[12] Havelock T J 1926 Forced surface waves on water *Phil. Mag.* **8** 569–76
[13] Milner S T 1991 Square patterns and secondary instabilities in driven capillary waves *J. Fluid Mech.* **225** 81–100
[14] Craik A D D and Armitage J 1995 Faraday excitation, hysteresis and wave instability in a narrow rectangular wave tank *Fluid Dyn. Res.* **15** 129–43
[15] Decent S P 1995 Hysteresis and mode competition in Faraday waves *PhD Thesis* University of St Andrews
[16] Decent S P and Craik A D D 1997 On limit cycles arising from the parametric excitation of standing waves *Wave Motion* **25** 275–94
[17] Miles J W 1994 Faraday waves, rolls versus squares *J. Fluid Mech.* **269** 353–71
[18] Decent S P and Craik A D D 1995 Hysteresis in Faraday resonance *J. Fluid Mech.* **293** 237–68
[19] Decent S P and Craik A D D 1999 Sideband instability and modulations in Faraday waves *Wave Motion* **30** 43–55
[20] Chen P and Vinals J 1997 Pattern selection in Faraday waves *Phys. Rev. Lett.* **79** 2670–3
[21] Zhang W and Vinals J 1997 Pattern formation in weakly damping parametric surface waves *J. Fluid Mech.* **336** 301–30
[22] Miles J W and Henderson D 1990 Parametrically forced surface waves *Annu. Rev. Fluid Mech.* **22** 143–65
[23] Muller H W 1993 Periodic triangular pattern in the Faraday experiment *Phys. Rev. Lett.* **71** 3287–90
[24] Huntley I 1972 Observations on a spatial-resonance phenomenon *J. Fluid Mech.* **53** 209–16
[25] Mahony J and Smith R 1972 On a model representation for certain spatial resonance phenomena *J. Fluid Mech.* **53** 193–208
[26] Yoshimatsu K and Funakoshi M 2001 Surface waves in a square container due to resonant horizontal oscillations *J. Phys. Soc. Japan* **70** 394–406
[27] Brunnhofer H M 2005 Forced capillary–gravity water waves in a 2D rectangular basin *PhD Thesis* Virginia Polytechnic Institute and State University
[28] Joseph D D 2003 Viscous potential flow *J. Fluid Mech.* **479** 191–7
[29] Joseph D D and Wang J 2004 The dissipation approximation and viscous potential flow *J. Fluid Mech.* **505** 365–77
[30] Joseph D D 2006 Potential flow of viscous fluids: historical notes *Int. J. Multiph. Flow* **32** 285–310
[31] Hubbard J H and West B H 1991 *Differential Equations: A Dynamical Systems Approach* part I (New York: Springer)